

Absolute clock synchronization with a single time-correlated photon pair source over a 10 km optical fibre

JIANWEI LEE,¹ LIJIONG SHEN,¹ ADRIAN NUGRAHA UTAMA,¹ AND CHRISTIAN KURTSIEFER^{1,2,*}

¹Centre for Quantum Technologies, National University of Singapore, 3 Science Drive 2, Singapore 117543, Singapore

²Department of Physics, National University of Singapore, 2 Science Drive 3, Singapore 117551, Singapore

*christian.kurtsiefer@gmail.com

Abstract: We demonstrate a point-to-point clock synchronization protocol based on bidirectionally propagating photons generated in a single spontaneous parametric down-conversion (SPDC) source. Tight timing correlations between photon pairs are used to determine the single and round-trip times measured by two separate clocks, providing sufficient information for distance-independent absolute synchronization secure against symmetric delay attacks. We show that the coincidence signature useful for determining the round-trip time of a synchronization channel, established using a 10 km telecommunications fiber, can be derived from photons reflected off the end face of the fiber without additional optics. Our technique allows the synchronization of multiple clocks with a single reference clock co-located with the source, without requiring additional pair sources, in a client-server configuration suitable for synchronizing a network of clocks.

© 2022 Optical Society of America under the terms of the [OSA Open Access Publishing Agreement](#)

1. Introduction

Complementary to clock recovery schemes from data streams, absolute clock synchronization protocols, e.g. network time protocol (NTP), precision time protocol (PTP), two-way satellite time transfer (TWSTT), are widely-used to determine the offset between physically separated clocks [1–4]. By exchanging counter-propagating signals, and assuming a symmetric synchronization channel, parties estimate one-way propagation delays as half the round-trip time signals without characterizing their physical separation beforehand. Spatially separated parties then deduce their absolute clock offset by comparing signal propagation times measured with their devices with the expected propagation delay [5]. Recently, protocol implementations with entangled photon pairs suggest securing the synchronization channel by measuring non-local correlations – a technique inspired by entanglement-based quantum key distribution (QKD) [6–8]. With independent hydrogen-maser and rubidium clocks as references, the protocol has a demonstrated timing stability limited to the intrinsic instability of the clocks over 7 km [9], and is secure against symmetric-delay attacks [6]. However, to realize a bidirectional exchange of photons, these demonstrations required a photon pair source at each end of the synchronization channel, posing a resource challenge when synchronizing multiple clocks.

In this work, we experimentally demonstrate a bidirectional clock synchronization protocol where the synchronization channel is established with a 10 km optical fiber and a single entangled photon pair source. The round-trip time is sampled using time-correlation measurements between the detection times of photon pairs, with one photon of the pair back-reflected at the remote side using the end face of the fiber. We demonstrate a distance-independent synchronization of two separated clocks, referenced to independent rubidium frequency standards. Already from a quite modest photon pair detection rate of 160 s^{-1} we obtain a precision sufficient to resolve clock

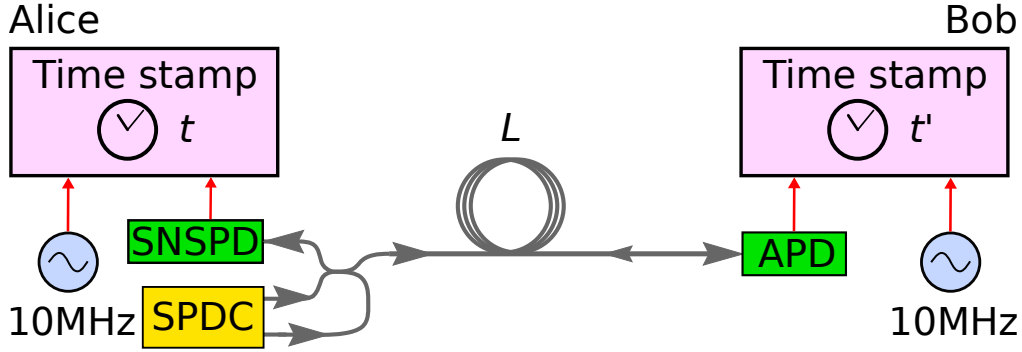


Fig. 1. Clock synchronization setup. Alice has a source of time-correlated photon pairs based on spontaneous parametric down-conversion (SPDC) and a single-photon nanowire photodetector (SNSPD). One photon of the pair is detected locally, while the other one is sent through a single mode fiber of length L to be detected on the remote side with Bob's InGaAs avalanche photodiode (APD). Times of arrival for all detected photons are recorded at each side with respect to the local clock, each locked to a rubidium frequency reference (10 MHz). Occasionally, a transmitted photon is reflected at the end face of the fiber back to Alice, allowing her to determine the round-trip time and derive the absolute offset between the clocks.

offset fluctuations with an uncertainty of 88 ps in 100 s, consistent with the intrinsic frequency instability between our clocks.

2. Time synchronization protocol

The protocol involves two parties, Alice and Bob, connected by a single mode optical fiber (see Fig. 1). Alice has an SPDC source producing photon pairs, one photon is detected locally, while the other is sent and detected on the remote side. Occasionally, the transmitted photon undergoes Fresnel reflection ($R \approx 3.5\%$) at the end face of the fiber, and is eventually detected by Alice instead. Every photodetection event is time tagged according to a local clock which assigns time stamps t and t' at Alice and Bob, respectively.

Photon pairs emerging from SPDC are tightly time-correlated (≈ 100 fs) [10]. Thus, for an offset δ between the clocks, a propagation time Δt_{AB} from Alice to Bob, and Δt_{BA} in the other direction, the second-order correlation function [11] $G^{(2)}(\tau)$ of the time difference $\tau = t' - t$ has a peak at

$$\tau_{AB} = \delta + \Delta t_{AB} \quad (1)$$

due to pairs detected at opposite ends of the channel, whereas for two photons detected by Alice at t and $t + \tau$, the auto-correlation function $R(\tau)$ will show a peak at

$$\tau_{AA} = \Delta t_{AB} + \Delta t_{BA}, \quad (2)$$

corresponding to the round-trip time of the channel. If the propagation times in the two directions are the same, $\Delta t_{AB} = \Delta t_{BA}$, the clock offset can be deduced directly from the positions of the two peaks using

$$\delta = \tau_{AB} - \frac{1}{2} \tau_{AA}, \quad (3)$$

independently of the propagation time Δt_{AB} . In this way, the protocol is inherently robust against symmetric changes in channel propagation times.

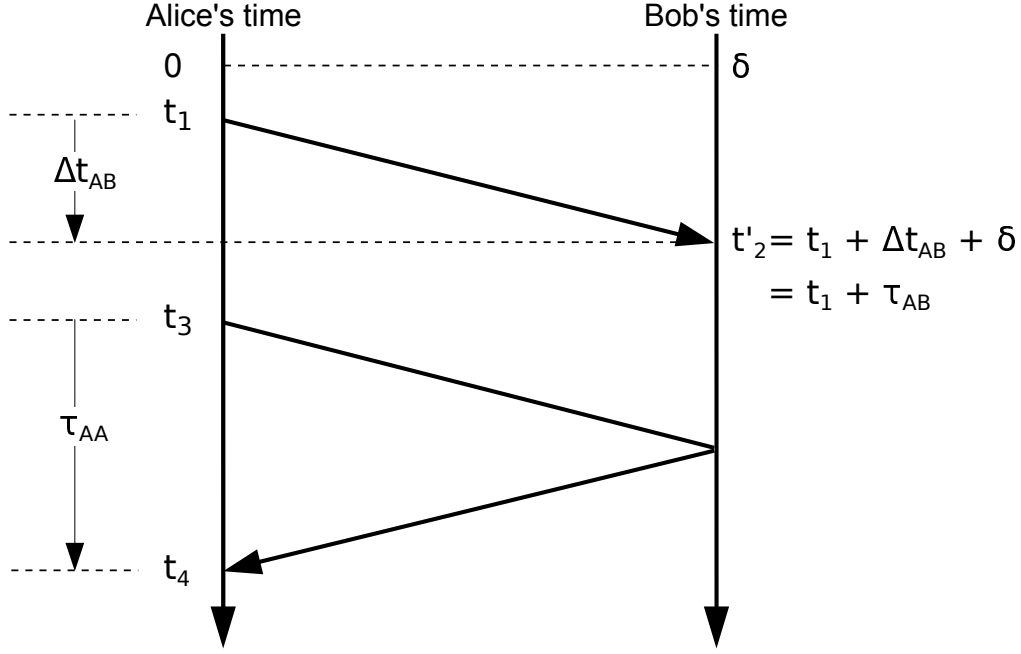


Fig. 2. Clock synchronization scheme. Alice and Bob measure detection times t and t' of photon pairs generated from Alice's source using local clocks. Detection times t_1 and t'_2 are associated with a time-correlated photon pair where one photon of the pair is transmitted to Bob, while t_3 and t_4 are associated with a pair where one of the photons is reflected at Bob back to Alice. The single-trip time τ_{AB} of photons in the synchronization channel, calculated from the time difference $t'_2 - t_1$, depends on the signal delay Δt_{AB} associated with the length of the channel, and the absolute clock offset δ between the clocks. The round-trip time τ_{AA} of the channel is estimated using $t_4 - t_3$. Assuming a symmetric delay channel, δ can be derived from τ_{AB} and τ_{AA} without *a priori* knowing Δt_{AB} .

3. Experiment

A sketch of the experimental setup is shown in Fig. 1. Our photon pair source [12–14] is based on Type-0 SPDC in a periodically-poled crystal of potassium titanyl phosphate (PPKTP) pumped by a laser diode at 658 nm (Ondax, stabilized with holographic grating). The resulting photon pairs are degenerate at 1316 nm, close to the zero dispersion wavelength of the synchronization channel (SMF-28e, 10 km), with a bandwidth of ≈ 50 nm on either side of this wavelength [14]. Signal and idler photons are efficiently separated using a wavelength division demultiplexer (WDM). Fiber beam splitters separate the photon pairs so that one photon is detected locally with a superconducting nanowire single-photon detector (SNSPD, optimized for 1550 nm), while the other photon is routed into the synchronization channel where it is detected on the remote side with an InGaAs avalanche photodiode (APD). The SNSPD has relatively low jitter (≈ 40 ps) compared to APDs (≈ 300 ps), and allows Alice to measure the round-trip time more accurately regardless of the choice of detector by the remote party. With a pump power of 2.5 mW focused to a beam waist of $140 \mu\text{m}$ at the centre of the crystal, we observed pair rates of 160 s^{-1} and 8900 s^{-1} associated with the round-trip and single-trip propagation of photons, respectively.

Photon detection times t and t' at Alice and Bob are registered with a nominal resolution of ≈ 4 ps. We compute [15] the histograms $G^{(2)}(\tau)$ and $R(\tau)$ with a bin width of 62.5 ps, and

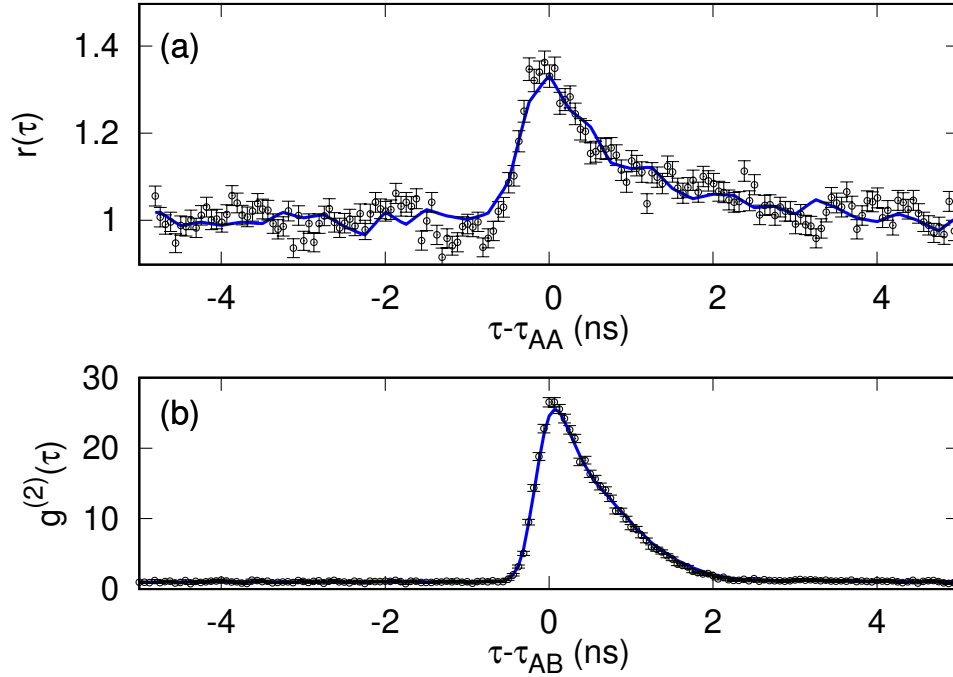


Fig. 3. Timing correlations showing coincidence peaks due to (a) round-trip and (b) single-trip propagation of photons in the synchronization channel. (a) $r(\tau)$: auto-correlation function $R(\tau)$ normalized to background coincidences extracted from Alice's timestamps acquired over 100 s. (b) $g^{(2)}(\tau)$: cross-correlation function $G^{(2)}(\tau)$ normalized to background coincidences extracted from Alice and Bob's timestamps acquired over 3 s. Solid lines: fits to heuristic model. τ_{AA} and τ_{AB} : peak positions of respective distributions. Error bars: propagated Poissonian counting statistics.

observed coincidence peaks associated with the single-trip and round-trip propagating photons (FWHM = 905 ps and 950 ps, respectively). Figure 3 shows the respective histograms normalized to background coincidences when the two clocks are locked to a common rubidium frequency reference (Stanford Research Systems FS725), separated by a fiber spool of constant length $L = 10$ km. To deduce the clock offset, we first generate empirical models (Fig. 3, solid-lines) for the two coincidence peaks using 100 s of timestamp data – the models are used to fit subsequent histograms to extract peak positions τ_{AB} and τ_{AA} . With the peak positions, we then determine the clock offset using Eqs. 2 and 3.

To characterize the synchronization precision δt as a function of the acquisition time, we measure the standard deviation of twenty offset measurements, each extracted from time stamps recorded for a duration T_a . Figure 4 shows the precision of the measured offset, single-trip (τ_{AB}) and round-trip times (τ_{AA}). We observe that the precision for the single and round-trip times improves with T_a for timescales $\lesssim 100$ s, but deteriorates for longer timescales. We attribute this effect to temperature-dependent ($\Delta T = 45$ mK over 1 min, 160 mK over 3 hours) length fluctuations, given that the propagation delay variation [16] of our fiber is several $10 \text{ ps km}^{-1} \text{ K}^{-1}$. However, we observe that these long-term fluctuations are suppressed in the clock offset measurement with the distance-independent synchronization protocol.

For subsequent demonstrations, we set $T_a = 3$ s and 90 s for the single and round-trip time measurements, obtaining a precision of 12 ps and 14 ps, respectively. Each 90 s window used

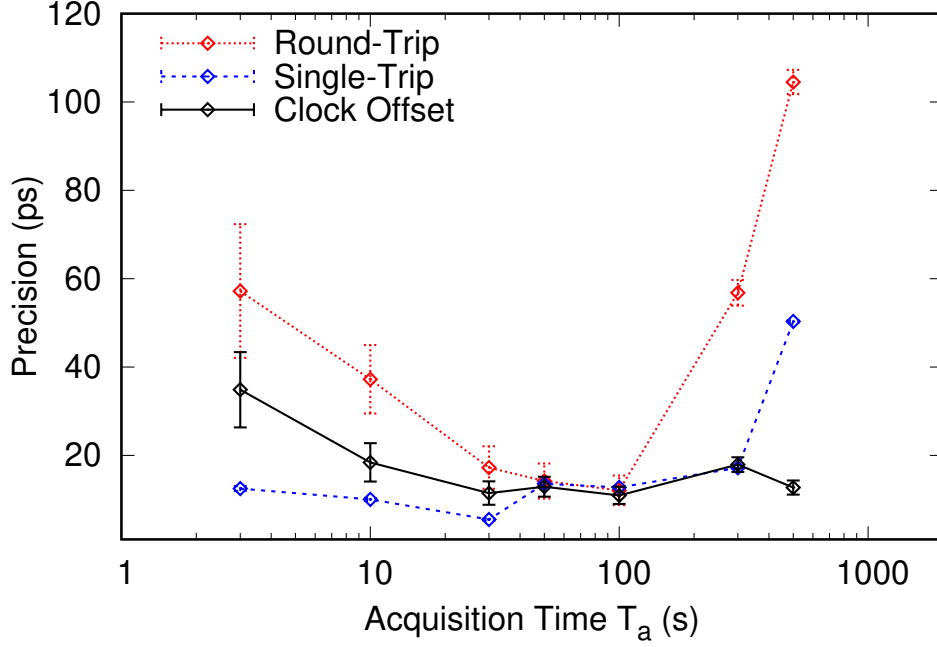


Fig. 4. Precision of the round-trip (red) and single-trip (blue) times, and the clock offset (black) between two clocks. Both clocks are locked to the same frequency reference. Error bars: precision uncertainty due to errors in determining the positions, τ_{AB} and τ_{AA} , of the coincidence peaks.

to evaluate the round-trip time thus contains thirty single-trip time measurements. For each single-trip time value, we evaluate the clock offset using the round-trip time evaluated in the same window. This results in a precision of 16 ps for the measured offset. Measuring the single-trip delay with shorter T_a enables frequent measuring of $G^{(2)}(\tau)$, and is useful for tracking the position of its coincidence peak (τ_{AB}) in the scenario where clocks are locked to independent frequency references.

The minimum resolvable clock separation associated with the offset precision is 3.3 mm. To demonstrate that the protocol is secure against symmetric channel delay attacks, we change the propagation length over several meters during synchronization — three orders of magnitude larger than the minimum resolvable length-scale.

4. Distance-independent clock synchronization with the same reference clock

To simulate a symmetric channel delay attack, we impose different propagation distances using different fiber lengths. Figure 5 shows the measured offset δ and the round-trip time ΔT , with an overall standard deviation of 26 ps, and an overall mean of $\bar{\delta}$. The sets of δ obtained for $L = L_0 + 1$ m and $L_0 + 10$ m, with mean offsets $\bar{\delta} - 24(17)$ ps, and $\bar{\delta} + 20(20)$ ps, respectively, show significant overlap with those obtained with $L = L_0 = 10$ km with mean offset $\bar{\delta} + 1(17)$ ps. Comparing the additional mean offset of 19(26) ps to the additional single-trip delay (48.3 ns) expected for extending our optical channel from $L = L_0$ to $L_0 + 10$ m, our protocol suppresses the contribution of the additional propagation delay on the measured offset by a factor of $\approx 4 \times 10^{-4}$.

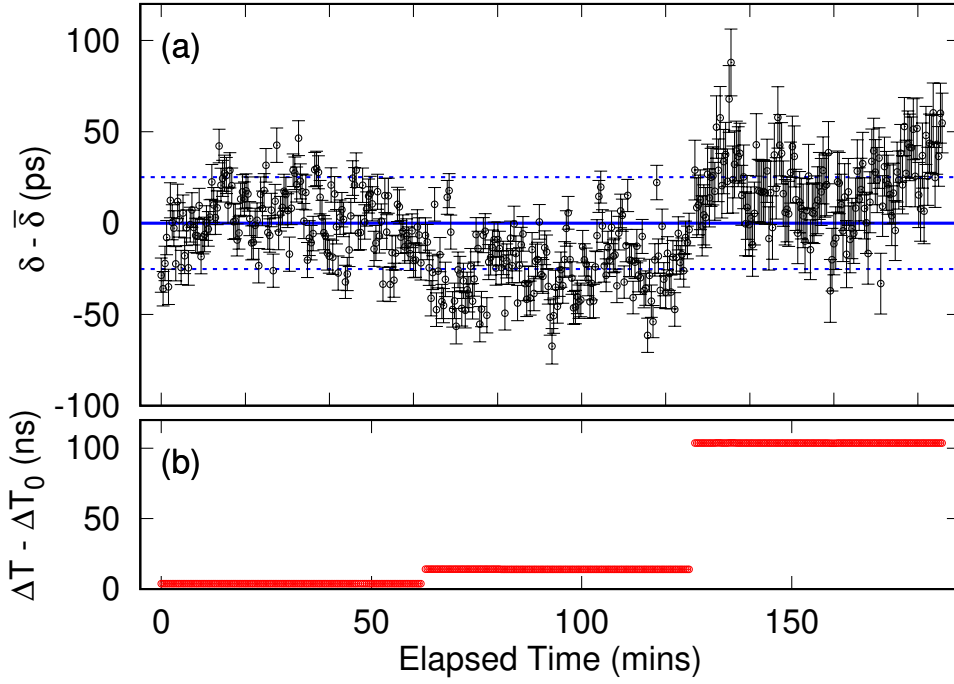


Fig. 5. (a) Measured offset δ between two clocks, both locked on the same frequency reference. The continuous line indicates the average offset $\bar{\delta}$. Error bars: precision uncertainty due to errors in determining the positions, τ_{AB} and τ_{AA} , of the coincidence peaks. Dashed lines: one standard deviation. (b) The round-trip time ΔT was changed using fiber lengths $L = L_0 = 10$ km, $L_0 + 1$ m, and $L_0 + 10$ m. $\Delta T_0 = 103.3 \mu\text{s}$.

120 5. Distance-independent clock synchronization with independent clocks

121 To examine a more realistic scenario, we provide each time-stamping unit with an independent
 122 frequency reference (both Stanford Research Systems FS725), resulting in a clock offset that
 123 drifts with time $\delta \rightarrow \delta(t)$.

124 The frequency references each have a nominal frequency accuracy $d_0 < 5 \times 10^{-11}$, resulting in
 125 a relative accuracy $\sqrt{2} d_0$ between two clocks. We evaluate the offset from the time stamps every
 126 $T_a = 3$ s so that the maximum expected drift (< 212 ps) of the coincidence peak in $G^{(2)}(\tau)$ is
 127 smaller than its FWHM. This pseudo-stationary regime allows the peak positions to be extracted
 128 with the same fitting procedure used when the clocks are locked onto the same frequency
 129 reference [6].

130 We again simulate a symmetric channel delay attack using three different values of L . Figure 6
 131 shows the measured $\delta(t)$ which appears to follow a continuous trend over different round-trip
 132 times, indicating that the delay attacks were ineffective. Discontinuities in $\delta(t)$ correspond to
 133 periods when fibers were changed.

134 To verify that meaningful clock parameters can be extracted from $\delta(t)$ despite the attack, we
 135 fit the data to a parabola $a t^2 + d t + b$, where a , d and b represent the relative aging, frequency
 136 accuracy and bias of the frequency references, respectively [17]. The resulting relative frequency
 137 accuracy between the clocks, $d = 5.1654(7) \times 10^{-11}$, agrees with the nominal relative frequency
 138 accuracy $\sqrt{2} d_0$ between our frequency references. The residual of the fit, $r(t)$ (Fig. 6(b)),
 139 fluctuates [18] (Allan deviation = 2.2×10^{-12} , time deviation = 88 ps in 100 s) mainly due to the
 140 intrinsic instabilities of our frequency references (2×10^{-12} in 100 s each).

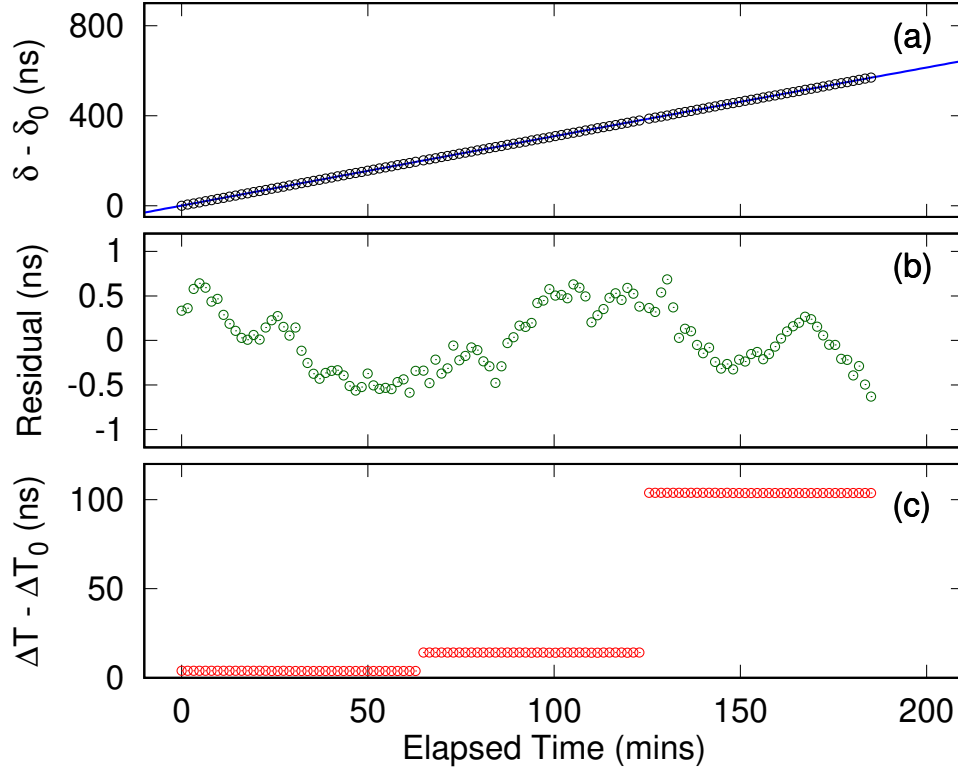


Fig. 6. (a) Measured offset δ between two clocks with different frequency references. Each value of δ was evaluated from measuring photon pair timing correlations for 3 s. The offset measured at the beginning is δ_0 . Continuous blue line: fit used to extract the relative frequency accuracy ($\approx 5.16 \times 10^{-11}$) between the clocks. (b) Residual of the fit fluctuates due to the intrinsic instability of the individual frequency references. (c) The round-trip time ΔT was changed using three different fiber lengths.

141 6. Protocol Security

142 Although not demonstrated in this work, Alice and Bob can verify the origin of each photon by
 143 synchronizing with polarization-entangled photon pairs and performing a Bell measurement to
 144 check for correspondence between the local and transmitted photons. This proposal addresses
 145 the issue of spoofing in current classical synchronization protocols [6, 8]. However, due to low
 146 coincidence-to-accidental ratio associated with the round-trip time measurement (CAR=0.13),
 147 this authentication scheme is only feasible for the single-trip time measurement (CAR=8.9).
 148 Consequently, users can only authenticate photons traveling from Alice to Bob, and have to
 149 assume that the synchronization channel has not been asymmetrically manipulated in order to
 150 incorporate the round-trip time measurement in the clock offset calculation (Eqn. 3).

151 In addition, we also assumed that the photon propagation times in both directions were equal
 152 ($\Delta t_{AB} = \Delta t_{BA}$). Without this assumption, the offset

$$\delta = \tau_{AB} - \tau_{AA} + \Delta t_{BA} \quad (4)$$

153 can no longer be obtained directly from the peak positions τ_{AB} and τ_{AA} .

154 We note that an adversary will be able to exploit both assumptions while evading detection by

passively rerouting photons traveling in opposite directions in the synchronization channel without disturbing their polarization states [19]. This attack is based on the fact that the momentum and polarization degree-of-freedom of our photons are separable, and remains a security loophole in similar implementations [6, 7].

7. Conclusion

We have demonstrated a protocol for synchronizing two spatially separated clocks absolutely with time-correlated photon pairs generated from SPDC. By assuming symmetry in the synchronization channel, the protocol does not require *a priori* knowledge of the relative distance or propagation times between two parties, providing security against symmetric channel delay attacks and timing signal authentication via the measurement of a Bell inequality [8]. Compared to previous implementations [6, 7], our protocol requires only a single photon pair source, relying on the back-reflected photon to sample the round-trip time of the synchronization channel. This arrangement allows multiple parties to synchronize with bidirectional signals with a single source.

With our protocol, we synchronize two independent rubidium clocks while changing their relative separation, using telecommunication fibers of various lengths (≥ 10 km) as a synchronization channel. Even with relatively modest detected coincidence rates (160 s^{-1}) used for the round-trip time measurement, we obtained a precision sufficient to resolve clock offset fluctuations with a time deviation of 88 ps in 100 s, consistent with the intrinsic frequency instabilities of our clocks. The precision improves with detectors with lower timing jitter [7], brighter sources, or for a transmission channel with insignificant dispersion (free space). Frequency entanglement may also be leveraged to cancel dispersion non-locally, improving protocol precision over optical channels in future work [7].

8. Backmatter

Funding. This research is supported by the National Research Foundation, Prime Minister's Office, Singapore and the Ministry of Education, Singapore under the Research Centres of Excellence programme.

Acknowledgments. We thank S-Fifteen Instruments for assistance with the entangled photon pair source and the InGaAs detector.

Disclosures. The authors declare no conflicts of interest.

Data availability. Data underlying the results presented in this paper are not publicly available at this time due to their large file size (about 310 Gb) but may be obtained from the authors upon reasonable request.

References

1. W. Wenjun, D. Shaowu, L. Huanxin, and Z. Hong, "Two-way satellite time and frequency transfer: Overview, recent developments and application," in *2014 European Frequency and Time Forum (EFTF)*, (IEEE, 2014), pp. 121–125.
2. D. L. Mills, "Internet time synchronization: the network time protocol," *IEEE Transactions on Commun.* **39**, 1482–1493 (1991).
3. "Ieee standard for a precision clock synchronization protocol for networked measurement and control systems," IEC 61588:2009(E) pp. C1–274 (2009).
4. P. Moreira, J. Serrano, T. Wlostowski, P. Loschmidt, and G. Gaderer, "White rabbit: Sub-nanosecond timing distribution over ethernet," in *2009 International Symposium on Precision Clock Synchronization for Measurement, Control and Communication*, (2009), pp. 1–5.
5. L. Narula and T. E. Humphreys, "Requirements for secure clock synchronization," *IEEE J. Sel. Top. Signal Process.* **12**, 749–762 (2018).
6. J. Lee, L. Shen, A. Cerè, J. Troupe, A. Lamas-Linares, and C. Kurtsiefer, "Symmetrical clock synchronization with time-correlated photon pairs," *Appl. Phys. Lett.* **114**, 101102 (2019).
7. F. Hou, R. Dong, R. Quan, X. Xiang, T. Liu, X. Yang, H. Li, L. You, Z. Wang, and S. Zhang, "Fiber-optic quantum two-way time transfer with frequency entangled pulses," arXiv preprint arXiv:1812.10077 (2018).
8. A. Lamas-Linares and J. Troupe, "Secure quantum clock synchronization," in *Advances in Photonics of Quantum Computing, Memory, and Communication XI*, vol. 10547 (International Society for Optics and Photonics, 2018), p. 105470L.

- 204 9. R. Quan, H. Hong, W. Xue, H. Quan, W. Zhao, X. Xiang, Y. Liu, M. Cao, T. Liu, S. Zhang *et al.*, "Implementation
205 of field two-way quantum synchronization of distant clocks across a 7 km deployed fiber link," arXiv preprint
206 arXiv:2109.00784 (2021).
- 207 10. C.-K. Hong, Z.-Y. Ou, and L. Mandel, "Measurement of subpicosecond time intervals between two photons by
208 interference," Phys. review letters **59**, 2044 (1987).
- 209 11. R. J. Glauber, "The quantum theory of optical coherence," Phys. Rev. **130**, 2529 (1963).
- 210 12. Y. Shi, S. M. Thar, H. S. Poh, J. A. Grieve, C. Kurtsiefer, and A. Ling, "Stable polarization entanglement based
211 quantum key distribution over metropolitan fibre network," arXiv preprint arXiv:2007.01989 (2020).
- 212 13. A. Lohrmann, C. Perumangatt, A. Villar, and A. Ling, "Broadband pumped polarization entangled photon-pair
213 source in a linear beam displacement interferometer," Appl. Phys. Lett. **116**, 021101 (2020).
- 214 14. J. A. Grieve, Y. Shi, H. S. Poh, C. Kurtsiefer, and A. Ling, "Characterizing nonlocal dispersion compensation in
215 deployed telecommunications fiber," Appl. Phys. Lett. **114**, 131106 (2019).
- 216 15. C. Ho, A. Lamas-Linares, and C. Kurtsiefer, "Clock synchronization by remote detection of correlated photon pairs,"
217 New J. Phys. **11**, 045011 (2009).
- 218 16. M. Bousonville and J. Rausch, "Velocity of signal delay changes in fibre optic cables," in *Proceedings of the Ninth
219 European Workshop on Beam Diagnostics and Instrumentation for Particle Accelerators (DIPAC)*, (2009).
- 220 17. G. Xu and Y. Xu, *GPS, Theory, Algorithms and Applications* (Springer Berlin Heidelberg, Berlin, Heidelberg, 2016).
- 221 18. W. J. Riley, *Handbook of frequency stability analysis* (US Department of Commerce, National Institute of Standards
222 and Technology, 2008).
- 223 19. J. Lee, L. Shen, A. Cerè, J. Troupe, A. Lamas-Linares, and C. Kurtsiefer, "Asymmetric delay attack on an
224 entanglement-based bidirectional clock synchronization protocol," Appl. Phys. Lett. **115**, 141101 (2019).